Injectable Bone Substitute Based on β-TCP Combined With a Hyaluronan-Containing Hydrogel Contributes to Regeneration of a Critical Bone Size Defect Towards Restitutio ad Integrum

Mike Barbeck, PhD[1,2]
Christiane Hoffmann, PhD[3]
Robert Sader, MD, DMD[1]
Fabian Peters, PhD[3]
Wolf-Dietrich Hübner, MD[3]
Charles James Kirkpatrick, MD, PhD[2]
Shahram Ghanaati, MD, DMD[1,2]*

In the present in vivo study, the regenerative potential of a new injectable bone substitute (IBS) composed of beta-tricalcium phosphate (β-TCP) and hyaluronan was tested in a rabbit distal femoral condyle model. To achieve this, 2 defects of 6 mm in diameter and 10 mm in length were drilled into each femur condyle in a total of 12 animals. For each animal, 1 hole was filled with the substitute material, and the other was left empty to serve as the control. After 1, 3, and 6 months, the regenerative process was analyzed by radiography as well as by histological and histomorphometrical analysis. The results revealed that bone tissue formation took place through osteoconductive processes over time, starting from the defect borders to the center. Both the β-TCP content and the hydrogel support bone tissue growth. The histomorphometrical measurements showed that the amount of bone formation in the experimental group was significantly higher compared with that found in the control group after 3 months (19.51 ± 5.08% vs. 1.96 ± 0.77%, $P < .05$) and 6 months (4.57 ± 1.56% vs. 0.23 ± 0.21%, $P < .05$). The application of the IBS gave a restitutio ad integrum result after 6 months and was associated with its nearly complete degradation, in contrast to the results found in the control group. In conclusion, the results of the present study demonstrate that the IBS contributes to sufficient bone regeneration by serving as a scaffold-like structure, combined with its degradation within 6 months.

Key Words: injectable bone substitute material, in vivo, bone regeneration, beta-tricalcium phosphate, hyaluronan

INTRODUCTION

In recent years, several injectable bone substitutes (IBS) based on calcium phosphates, combined with different natural-based polymers, such as cellulose and its derivatives, hyaluronic acid and other polymers, have been marketed as medical devices.[1–7] In addition to the injectable nature of the materials, the addition of these polymers to small-sized calcium phosphate granules has been shown to provide additional material features, such as hydroexpansibility to cover the defect borders and therewith an increase in osteoconductive bone growth.[2,5] In addition, there are advantages at the biological level, such as positively influencing osteoblastic growth, which enables the advancement of the material-mediated process of bone regeneration.[5–7] In a former preclinical in vivo study using the subcutaneous implantation model in Wistar rats, our group analyzed the tissue reactions and integration process, as well as the degradation behavior, of a new IBS.[8] This material is based on the above-mentioned substances, that is, crushed and sieved beta-tricalcium phosphate (β-TCP) granules, combined with a hydrogel containing the biocompatible compound hyaluronan as well as water. The data obtained in this in vivo study showed that the injectable paste-like material served as a stable and barrier-like structure over a period of at least 60 days within the subcutaneous tissue of rats, without allowing premature cell and tissue invasion inside the central implant regions. Furthermore, material degradation was shown to take place from the peripheral area toward the center of the implantation bed over time and was

[1] Department for Oral, Cranio-Maxillofacial and Facial Plastic Surgery, Medical Center of the Goethe University Frankfurt, Frankfurt am Main, Germany.
[2] REPAIR-Lab, Institute of Pathology, University Medical Center, Johannes Gutenberg University, Mainz, Germany.
[3] Curasan AG, Frankfurt Plant, Frankfurt am Main, Germany.
* *Corresponding author,* e-mail: shahram.ghanaati@kgu.de
DOI: 10.1563/aaid-joi-D-14-00203

associated with mononuclear cells as well as multinucleated giant cells. The latter cell type has been shown not to be induced by the small-sized β-TCP granules alone but rather by the multi-phase composition of the injectable bone substitute. Additionally, the implantation beds of the paste-like material showed relatively high vascularization, which has been shown to be an important factor in bone tissue regeneration.[9,10] In conclusion, the application of the new IBS, which showed integration and degradation behavior in accordance with the concept of the guided tissue/bone regeneration (GTR/GBR), was estimated to be an optimal bone substitute for bone regeneration.[11] In the present study, we performed the first test of the performance of the same IBS within a critical-sized bone model in the distal femur condyle of rabbits to confirm the data acquired in the former animal study. In this context, the overall goal was to assess the bone regenerative potential of the material and its regenerative performance within bone tissue.

Materials and Methods

Biomaterial

The analyzed injectable bone substitute (IBS) based on pure-phase beta-tricalcium phosphate (β-TCP) powder was synthesized by a solid-state reaction as previously described,[12] followed by milling and sieving steps to obtain β-TCP particles with a size of <63 μm. These particles were mixed with an organic porogen substance, which disappeared after a second sintering step ($\geq$1000°C), and subsequently compacted. After these preparations, the porous material was grinded and sieved to obtain ceramic particles with a size <63 μm, which provide the basis for the IBS. The β-TCP powder particles were formulated using an aqueous polymer solution comprised of modified cellulose and sodium hyaluronate to reach a powder to liquid ratio of $\geq$70%. Finally, the resulting viscoplastic paste-like bone substitute material was filled into syringes and sterilized by steam at 121°C for 15 minutes. The material was fabricated and provided by the curasan AG (Kleinostheim, Germany).

Experimental animals

In total, 12 six-month-old adult male New Zealand White rabbits were used to conduct the present in vivo study at the PharmaLegacy Laboratories (Shanghai SLAC Laboratory Animal Co, Ltd, Shanghai, China) after approval by the local animal ethics commission. The rabbits were assigned to treatment groups by the randomization function in a BioBook database system based on their body weights.

For defect generation, both distal femoral condyles of each animal were prepared. Thus, each rabbit was randomly assigned 1 implant and 1 unfilled drill hole/empty defect (control group). The animals were housed in standard stainless steel rabbit cages measuring 815 mm × 500 mm × 340 mm with 1 rabbit per cage. The animals were acclimatized for approximately 1 week prior to the commencement of the experimental procedures. The air in the room in which the animals were housed was filtered at a rate of 10–20 air changes per hour. The temperature was maintained at 16–26°C with a relative humidity of 40–70%. The temperature and humidity were continuously monitored, and the daily minimums and maximums were recorded. The room was illuminated with fluorescent light at cycles of 12 hours of light (8:00–20:00) and 12 hours of dark. The animals had ad libitum access to rabbit food (irradiated, Shanghai SLAC Laboratory Animal Co, Ltd) and tap water.

Surgery

Prior to the surgical procedure, the rabbits were sedated using a combination of ketamine (20–60 mg/kg, i.m.) and xylazine (1–5 mg/kg, i.p.). The animals were then additionally exposed to isoflurane in oxygen (0.5–5%) anesthesia. All of the surgical procedures were performed under strict asepsis. An incision of approximately 5 cm in length was made in the lateral skin of the distal femur, and the muscles were bluntly dissected to expose the distal femur condyle. Subsequently, a hole with a diameter of 6 mm and a length of 10 mm (representing a so-called "critical size defect") was drilled with a rose-head bur as the drill bit under irrigation with a sterile syringe, using sterile saline as bone-site coolant during drilling. The IBS was randomly inserted into each side of the distal femoral transcondylar drill-hole defects. The fascia was then closed over the filled or empty defect with a single uninterrupted suture, and the skin was prepared with wound clips. The surgical incision was bandaged to give protection.

Postoperatively, all of the animals were monitored on a daily basis for signs of ill health and general reaction to surgery and treatment. Over the postoperative course, when pain signs persisted, the rabbits received pain medication using buprenorphine (0.05 mg/kg, i.m. per day) and an antibiotic treatment using gentamicin (20 mg/kg, i.m.) after surgery. All exceptions to normal healthy appearance and behavior were recorded and detailed in standard clinical observation forms. Finally, the animals were sacrificed after 1, 3, or 6 months, and tissue samples were collected.

Explantation procedure, radiography, and histological workup

As the rabbits were sacrificed after 1, 3, or 6 months, tissue sections were collected, and both distal femoral condyles were dissected. Initial radiographs were taken after each rabbit was killed, and the collected samples were then used for histological preparation The latter included fixation in 10% neutral buffered formalin, undecalcified embedding in methyl methacrylate, further sectioning by a microtome, and staining of one section from each block with toluidine blue (pH 6.5). These slides were used for further qualitative histological evaluation and histomorphometrical analysis.

Histopathological evaluation and histomorphometrical measurements

The qualitative histological analyses were performed following an established and published standardized study protocol in which the focus was on analysis of the tissue reactions to the bone substitute and the morphology of bone healing achieved with the paste-like biomaterial.[8,13–18] Two independent investigators (SG and MB) analyzed the tissue reactions using an

Eclipse 80i histological microscope (Nikon, Tokyo, Japan). Microphotographs were acquired via a connected Nikon DS-Fi1 digital camera and a digital sight control unit (Nikon).

For the histomorphometrical analysis, "total scans"—that is, images of the total implantation beds of the IBS and the corresponding peri-implant tissue—were recorded at ×100 magnification via an Eclipse 80i histological microscope. This was combined with a DS-Fi1 digital camera and an automatic scanning table (Prior, Rockland, Md), connected to a computer with NIS-Elements 4.0 software (Nikon), following the protocol of a published method.[13–18] The NIS-Elements software enabled the quantification of the extent of newly formed bone in the defect region, as previously described.[13–18] In brief, the sizes of the total implantation beds and of the newly formed bone tissue were determined via the "area tool" of the category "Annotations and Measurements" of the software (in μm^2). These values allowed the calculation of the percentage of newly formed bone tissue within the defect areas in each animal. Additionally, the trabecular thickness of the new bone within the defect areas was measured via the NIS-Elements software (in μm). Thus, the "length tool" of the research software category "Annotations and Measurements" was used to measure the thickness of the bone trabeculae at different sites (as many as 10 different locations), enabling the comparison of trabecular thickness at the different time points and among the study groups.

Statistics

An unpaired *t* test was performed after assessing the differences between groups using the SPSS 16.0.1 software (SPSS Inc, Chicago, Ill) assuming a normal Gaussian distribution. Statistical significances were reported as significant (*) at $P > 0.05$. The significance of both intergroup (*) and intragroup (•) differences was quantified. The quantitative data are presented as the means ± standard deviations (SD).

Results

Throughout the investigation period, no macroscopic signs of inflammation were observed in any of the experimental animals. Furthermore, no signs of allergic or foreign body reactions were noted, and all of the animals survived the experimental course without complications.

Radiological results

To investigate the performance of the recently developed injectable bone void filler, a rabbit distal femoral condyle model was used. Defects of critical size were created and subsequently filled with the IBS (Figure 1a through c) or left empty to serve as a control (Figure 1d through f). The healing process was monitored by X ray at 1, 3, and 6 months after surgery.

The radiographic analyses showed that the IBS was visible after 1 month as a radiopaque dense bulk material (Figure 1a). Newly formed bone tissue was also identifiable in the peripheral areas of the defects, whereas the center appeared free of bone (Figure 1a). Three months after implantation, the IBS was still detectable within the defect areas, whereas new bone tissue with a trabecular structure was detected within the peripheral defect regions (Figure 1b). Furthermore, the evaluation of the center of the defects showed a radiopaque bulk, which hinted at a massive bone ingrowth at this time point (Figure 1b). Six months after implantation, the radiological evaluation of the regenerative process revealed no signs of the former defect within the cancellous bone tissue of the femoral head in the group of the IBS (Figure 1c). A dense network of bony trabeculae was observed in the areas of the former bone defects, and this network did not differ from the tissue structure of the surrounding unaffected cancellous bone tissue (Figure 1c).

In contrast, the empty defects of the controls showed only marginal new trabecular bone formation after one and three months (Figure 1d and e). Six months after treatment, a preliminary network of cancellous bone was observable within the former defect area, but this network did not exhibit the same trabecular density compared with the surrounding unaffected cancellous bone tissue (Figure 1f).

Histological results of bone healing

Histological Results of the IBS Group

One month after surgery, the implantation bed of the IBS was clearly circumscribed (Figure 2a). Undegraded β-TCP particles were still present within the complete defect areas (Figure 2a through c). Histological analysis revealed that a high amount of new calcified bony trabeculae was visible within the outer region of the implantation beds of the injectable bone substitute and derived from the neighboring unaffected bone tissue (Figure 2a). Within this outer region of the implantation bed adjacent to the defect borders, the calcified bone tissue presented a trabecular structure, and the β-TCP particles were incorporated within these trabeculae (Figure 2a and b).

In contrast to the findings related to the outer implant regions, only low amounts of newly built calcified bone tissue were found in the inner core of the implants (Figure 2a). In fact, uncalcified bone matrix was identified within this area of the implants (Figure 2c). Interestingly, this uncalcified bone matrix did not seem to have incorporated many β-TCP particles at this stage (Figure 2c). At this time point, within these inner regions of the implants, the β-TCP particles were mainly identified in close proximity to the uncalcified bone trabeculae but mostly not integrated within the newly built bone trabeculae, as observed in the outer implant regions (Figure 2c). Thus, the uncalcified bone matrix was mostly found between accumulations of β-TCP particles, where the hydrogel should be located (Figure 2c). However, the toluidine blue staining did not permit location of the hydrogel component involved in the growth of the newly built bone tissue.

Additionally, at this point, β-TCP particles were detected within the surrounding connective tissue of the bone trabeculae not involved in the growth of new bone tissue (Figure 2b through d). Thus, granulation tissue with the presence of granulocytes, lymphocytes, fibroblasts, macrophages, and multinucleated giant cells as well as a high amount of blood vessels was observed adjacent to those β-TCP particles not involved directly in bone regeneration (Figure 2d).

After three months, the implantation beds of the IBS were still detectable (Figure 3a). High amounts of newly built calcified bone tissue were found within the former outer

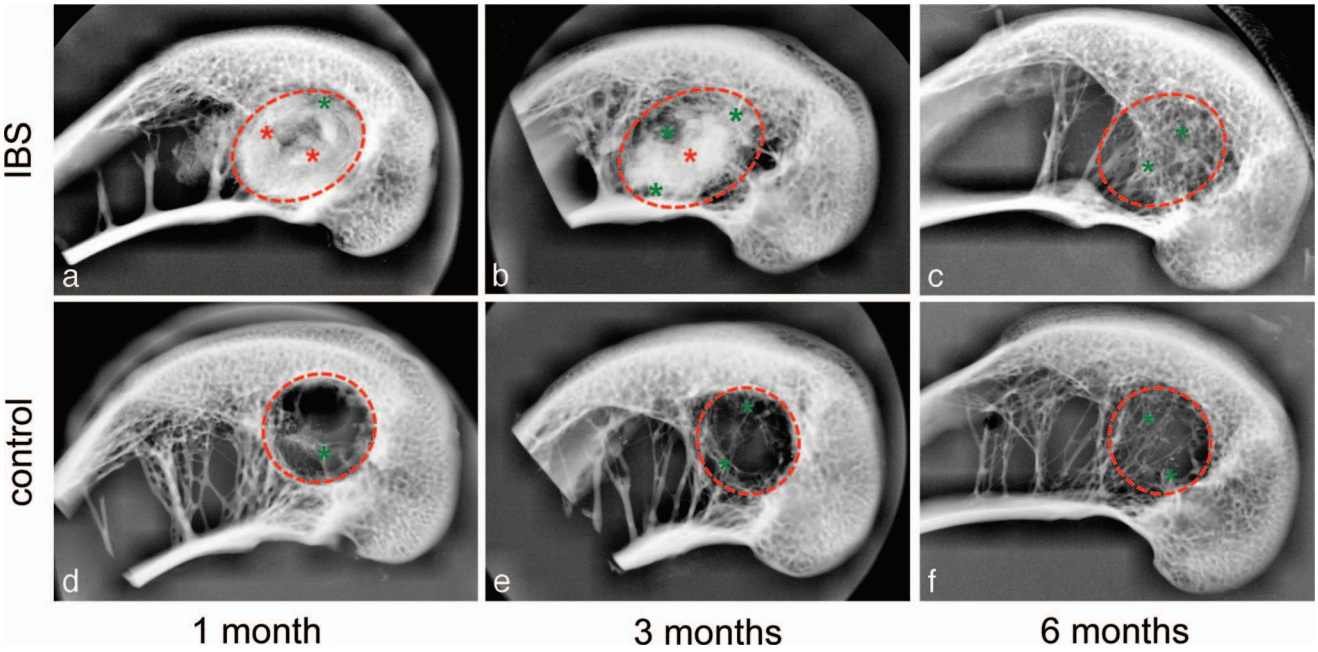

Figure 1. Radiological evaluation of the healing processes of the femoral bone defects treated with the injectable bone substitute (IBS) (a–c) and the control (d and f). (a) The radiographs show the implantation area of the IBS (red dashed line) 1 month after treatment. Within the implantation area, the principal observation was a bulk-like radiopaque mass (red asterisks) that appeared to represent the IBS. Within the peripheral defect regions, a trabecular bone tissue ingrowth (green asterisks) was seen at this time point, whereas the center of the implantation area seemed to be free of newly formed bone. (b) Three months after treatment, further regeneration of the trabecular bone structure (green asterisks) was observed within the peripheral regions of the defect area (red dashed line), whereas in the region of the implanted IBS a radiopaque center (red asterisks) was present, indicating massive bone ingrowth. (c) Six months after implantation, a normal trabecular bone structure (green asterisks) within the former defect area (red dashed line) was detectable, and no signs of the IBS could be found on radiography. (d) In the control group 1 month after treatment, the radiographs showed signs of trabecular bone ingrowth (green asterisk) within the peripheral regions of the former defect area (red dashed line). However, the majority of the defect area was free of bone. (e) Three months after treatment, only a few trabecular bone structures (green asterisks) were found within the control defect area (red dashed line), whereas the center of the defect area still lacked bone. (f) Six months after treatment, a rudimentary trabecular network (green asterisks) was detectable within the former defect area (red dashed line) but was not comparable to the dense structure of the neighboring cancellous bone tissue of the femoral head or the trabecular structure found in the group treated with the IBS at this time point.

implant region as well as within the former inner region of the implantation beds (Figure 3a). Thus, the newly built bone tissue featured a trabecular structure with interspaces but presented a denser structure compared with that of the bone tissue 1 month after application and the bone trabeculae in the unaffected regions (Figure 3a). Additionally, even the peripheral regions of the former implantation bed appeared to contain loosely dispersed bone trabeculae as well as fatty tissue, indicating that the regeneration process in these areas has been completed to the status of restitutio ad integrum (Figure 3a). High amounts of the β-TCP particles were still integrated within the new bone matrix (Figure 3b). Furthermore, approximately half of the β-TCP particles were found to be surrounded by a vessel-rich connective/granulation tissue adjacent to the areas where the bone matrix was found (Figure 3a through c). In these areas, the granules were still encircled mainly by mononuclear cells (such as macrophages) and a few multinuclear giant cells, showing further degradation of the bone substitute (Figure 3b).

Six months after surgery, only minor signs of the former implantation area of the IBS were detectable, whereas a nearly complete regeneration of the cancellous bone structure of the femoral condyles was detectable (Figure 4a). Most regions of the former implantation beds showed a bone tissue-specific composition, that is, bone trabeculae with osteocyte lacunae surrounded by fatty tissue, as was also seen in the untreated regions of the femoral condyles (Figure 4a). At this time, only a few remnants of the implanted β-TCP particles were found, mostly embedded within the calcified bone tissue of the implantation area (Figure 4b). Additionally, further bone matrix growth, incorporating the β-TCP particles, was detectable (Figure 4b). Low numbers of the β-TCP particles were also seen within the connective tissue, still surrounded by low amounts of granulation/connective tissue with macrophages and a few multinucleated giant cells (Figure 4c).

Histological Results of the Control Group

One month after treatment, only a limited amount of newly formed bone was detected in the empty defects of the control group, with most of the defect area containing fibrous tissue with fibroblast and adipocyte infiltration and moderate numbers of inflammatory cells (Figure 5a and b). Furthermore, no growth of an uncalcified bone matrix was found in the control group at this point. Three and 6 months after treatment, the defect areas were occupied mainly by fatty tissue, and only a very limited number of bony trabeculae were detectable (Figure 5c through

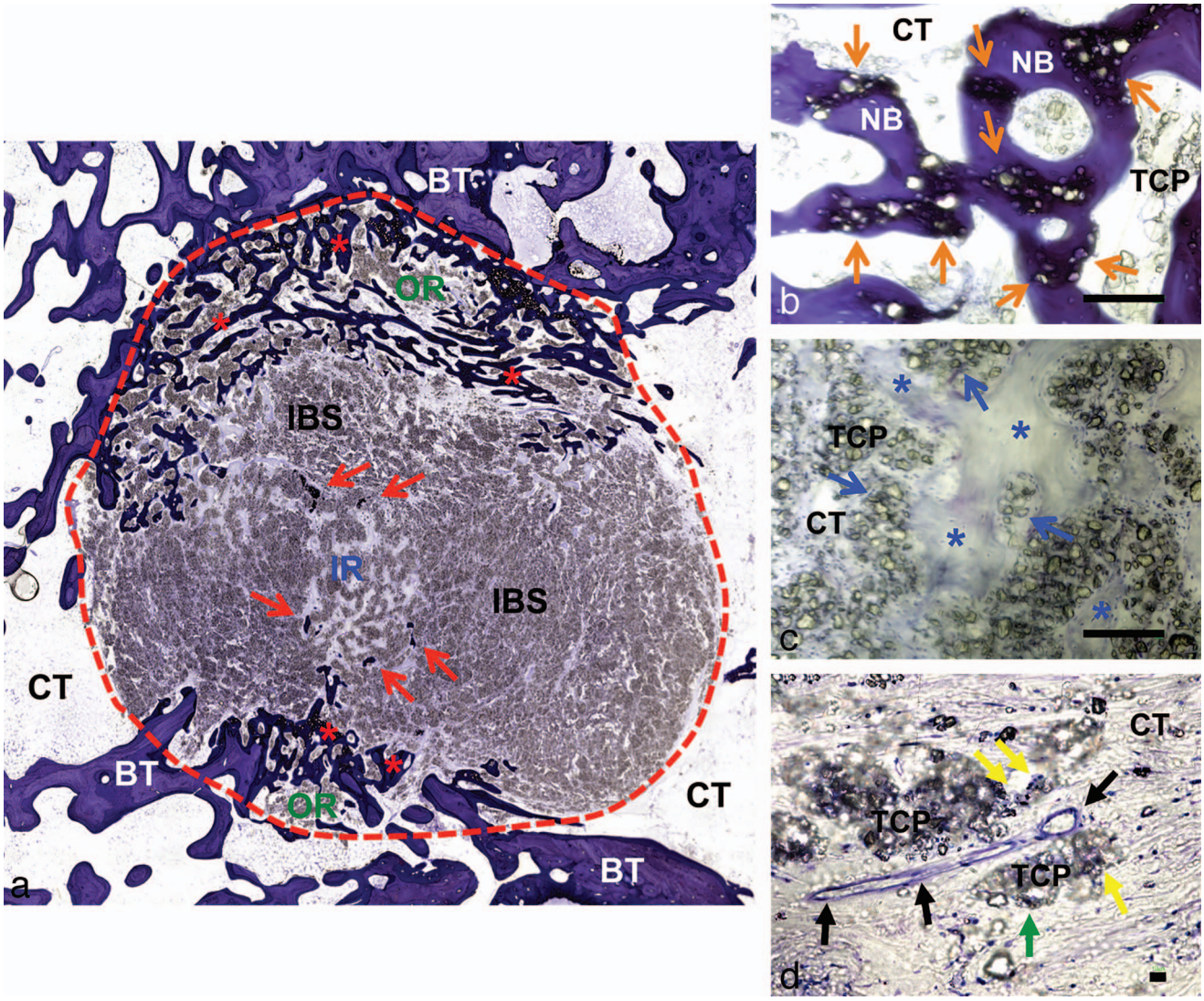

Figure 2. Histology of the bone defect treated with the injectable bone substitute (IBS) 1 month after implantation. (a) Overview of the implantation bed (red dashed line) of the IBS with an outer (OR) and inner implant region (IR). Within the OR, a high osteoconductive ingrowth of calcified bone tissue (red asterisks) was seen extending from the surrounding bone tissue (BT) towards the defect center. Within the IR, only low amounts of calcified bone tissue were visible (red arrows) (CT = connective tissue) ("total scan," toluidine blue staining, magnification ×100). (b) Newly formed calcified bone tissue (NB) is present in the outer region of the implantation bed of the IBS. The β-TCP particles (TCP) of the bone substitute were found integrated within the trabecular bone tissue (orange arrows) and within the surrounding connective tissue (CT) (toluidine blue staining, magnification ×200, scale bar = 100 μm). (c) Growth of uncalcified bone tissue (blue asterisks) is observed in the inner implant regions, and is mainly related to the interstices of the β-TCP particles (TCP). Groups of ceramic particles (blue arrows) are present as a scaffold structure (toluidine blue staining, magnification ×200, scale bar = 100 μm). (d) Tissue reaction to the IBS in the inner implant region. β-TCP particles were found embedded in a vessel-rich connective tissue (CT) surrounded by mononuclear (green arrows) and multinuclear cells (yellow arrows) (vessels = black arrows) (toluidine blue staining, magnification ×400, scale bar = 10 μm).

f). In conclusion, no bone tissue regeneration, and therefore no restitutio ad integrum, was observed in this study group up to 6 months after treatment (Figure 5e and f).

Histomorphometrical results

The histomorphometrical measurements of the bone volume in relation to the tissue volume (BV/TV, in %) showed similar values for animals treated with the IBS and the control group 1 month after surgery, and no significant differences were measured (IBS: 11.69 ± 1.32%, control: 11.15 ± 4.01%, Figure 6a). However, the histomorphometrical measurements did not include the area fraction of the uncalcified bone tissue that was detected by histology. This was based on the fact that the distinction of this tissue component from neighboring connective tissue was restricted due to a lack of contrast from the toluidine blue staining. Thus, the actual amount of newly built bone tissue was substantially higher at this early time point compared with the values obtained for the control group.

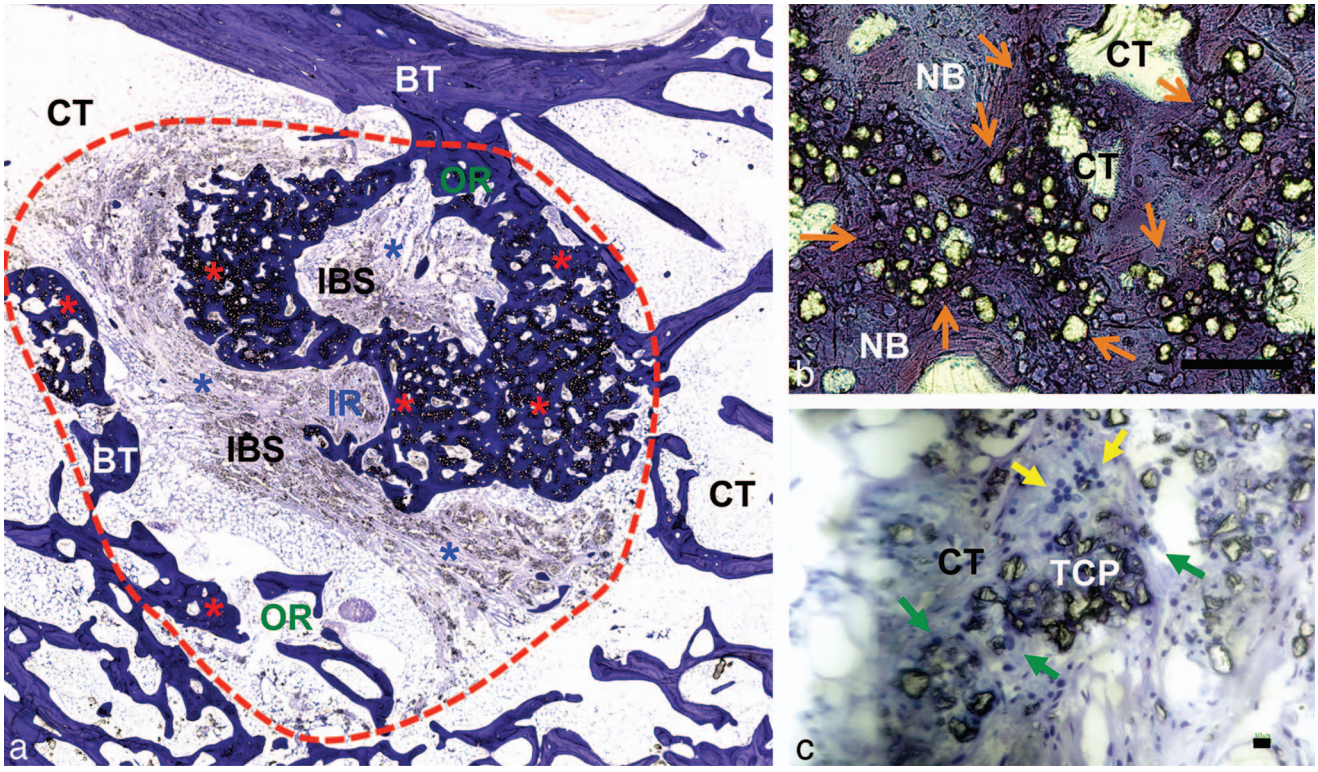

Figure 3. Histology in the group treated with the injectable bone substitute (IBS) 3 months after implantation. (a) Overview of the implantation bed (red dashed line) of the IBS. The former outer implant region (OR) as well as the former inner region (IR) now contain high amounts of newly formed dense bone tissue (red asterisks) with a bulk-like trabecular organization. Nonintegrated biomaterial in this bone tissue was surrounded by connective tissue (blue asterisks) (CT = connective tissue, BT = neighbored bone tissue) ("total scan," toluidine blue staining, magnification ×100). (b) This image shows the newly built bone tissue (NB) with its lamellar architecture, in which high amounts of the β-TCP particles (orange arrows) of the IBS are embedded (CT = connective tissue) (toluidine blue staining, magnification ×200, scale bar = 100 μm). (c) Shown are tissue reactions to the β-TCP particles (TCP) that were not involved in bone growth. These particles were embedded within a connective tissue (CT), and mononuclear (green arrows) and multinucleated cells (yellow arrows) were detectable at the surfaces of the particles (toluidine blue staining, magnification ×400, scale bar = 10 μm).

Three months after treatment, the measurements of the BV/TV ratio revealed that the bone volume within the defects filled with the IBS showed significant higher values compared with the control group (IBS: 19.51 ± 5.08%, control: 1.96 ± 0.77%, intergroup comparison: $P < .05$), while the bone volume values of the latter group showed a decreasing tendency compared with those found after 1 month, without intraindividual significance (Figure 6a). In addition, no significant differences in the bone volume was determined in the IBS group compared with those found after 1 month, although an increasing tendency was apparent (Figure 6a).

After 6 months, the BV/TV ratio was nearly twentyfold higher in the IBS group compared with the control group and thus significantly higher (IBS: 4.57 ± 1.56%, control: 0.23 ± 0.21%, intergroup comparison: $P < .05$, Figure 6a). In both study groups, a downward tendency for bone volume was apparent at this point, whereas only a significant increase in the bone volume was measurable in the IBS group (intragroup comparison: $P < .05$, Figure 6a).

The newly formed bone was further characterized by measuring the thickness of the bony trabeculae (in μm, Figure 6b). One month after treatment, both study groups showed similar values for the trabecular thickness without significant differences (IBS: 80.26 ± 2.99 μm, control: 90.08 ± 6.98 μm, Figure 6b). No measurement of the trabecular thickness of the uncalcified bone tissue was possible at this point because the contrast of toluidine blue staining did not permit separation of these tissue elements from the surrounding connective tissue.

Three months after treatment, a significant increase in the trabecular thickness was found in the IBS group (intragroup comparison: $P < .05$) but not in the control group, which showed a declining tendency without significant differences compared with that obtained one month after treatment (Figure 6b). Additionally, significant differences between the values of both study groups were measurable at this time point (IBS: 137.04 ± 10.77 μm, control: 66.47 ± 23.96 μm, intergroup comparison: $P < .05$, Figure 6b). Six months after treatment, declining tendencies in the trabecular thickness were measurable in both study groups, and a significant difference compared with the values obtained after 3 months was found only for the IBS group (intragroup comparison: $P < .05$, Figure 6b). Significant differences between the values of both study groups in regard to the trabecular thickness were still detectable, as the IBS group exhibited higher values (IBS:

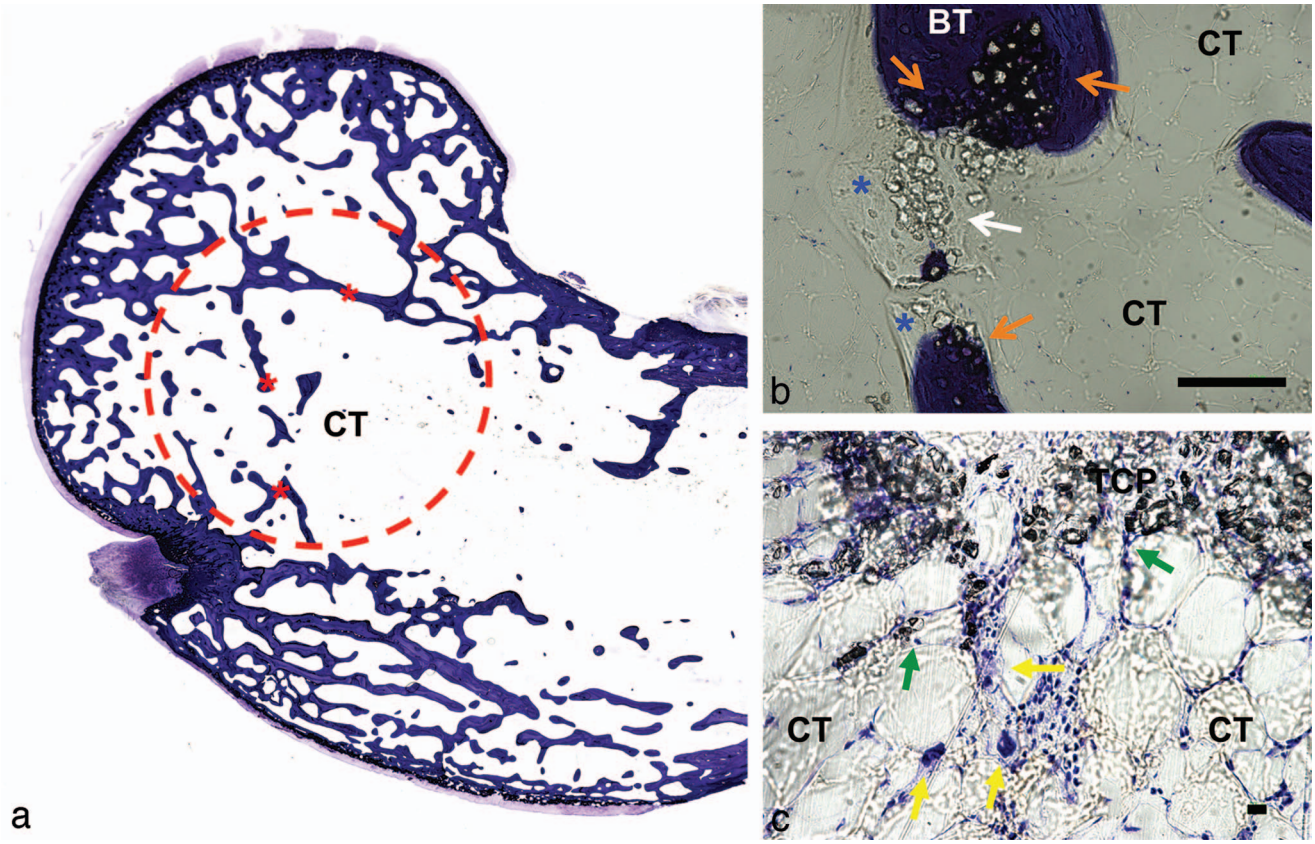

Figure 4. Histology of the bone healing mediated by the the injectable bone substitute (IBS) after 6 months. (a) Overview of a cross-section of the distal femur head. A trabecular network (red asterisks) was identifiable within the former defect area (red dashed line), and this network did not differ in its trabecular architecture and distribution compared with the surrounding healthy tissue (CT = connective tissue) ("total scan," toluidine blue staining, magnification ×100). (b) Only very low amounts of the β-TCP particles (orange arrows) of the IBS were found embedded within the trabeculae of the bone tissue (BT). Furthermore, a growth of uncalcified bone tissue (blue asterisks) was observable along the scattered accumulations of β-TCP particles (white arrow) within the former outer region of the implantation bed of the IBS (CT = connective tissue) (toluidine blue staining, magnification ×200, scale bar = 100 μm). (c) Only low amounts of the β-TCP particles (TCP) within the former implant area were embedded within connective tissue (CT) surrounded by mononuclear (green arrows) and multinuclear cells (yellow arrows) (toluidine blue staining, magnification ×400, scale bar = 10 μm).

92.84 ± 7.18 μm, control: 21.31 ± 19.73 μm, intergroup comparison: $P < .05$, Figure 6b).

Discussion

Injectable bone substitutes (IBS) have become an alternative to scaffolds or granular materials, as they can be administered in a minimally invasive way.[1–7] In addition, as generally expected from bone substitute materials, they should also function as an osteoconductive scaffold with a defined resorption rate and possess the required mechanical properties, to name a few of the requirements.[19]

Based on further findings, the combination of a hyaluronan hydrogel and β-TCP granules with a very high phase purity (>99%)—which has already been shown to allow complete regeneration of bone voids using granules of larger diameters—has been hypothesized to be an optimal biomaterial composite for an injectable bone substitute.[12,13] This assumption is also supported by data from previous in vivo studies of this novel IBS implanted subcutaneously and in tibial bone defects.[8,20] Briefly, material integration and degradation processes commenced from the periphery and reached the center of the implantation bed according to the concept of guided bone regeneration (GBR).[11] Additionally, a concomitantly high implant bed vascularization as a result of material-induced stimulation of multinucleated giant cells was demonstrated. This high level of vascularization, which is a key factor in a positive outcome of tissue regeneration,[9,10] is in large measure a result of the increased expression of the pro-angiogenic vascular endothelial growth factor by these multinucleated giant cells and has been substantiated in a further study conducted by our group.[13] In the current investigation, we tested the performance of the same IBS within a critical-sized bone defect model in the distal femur condyle of rabbits using radiological methods and histological and histomorphometrical analyses. The overall goal was to assess the regenerative potential of the bone substitute material and its performance in bone tissue regeneration.

Both the radiographic as well as the histological results of the present study showed that the IBS was detectable within critical-sized bone tissue defects up to 3 months after

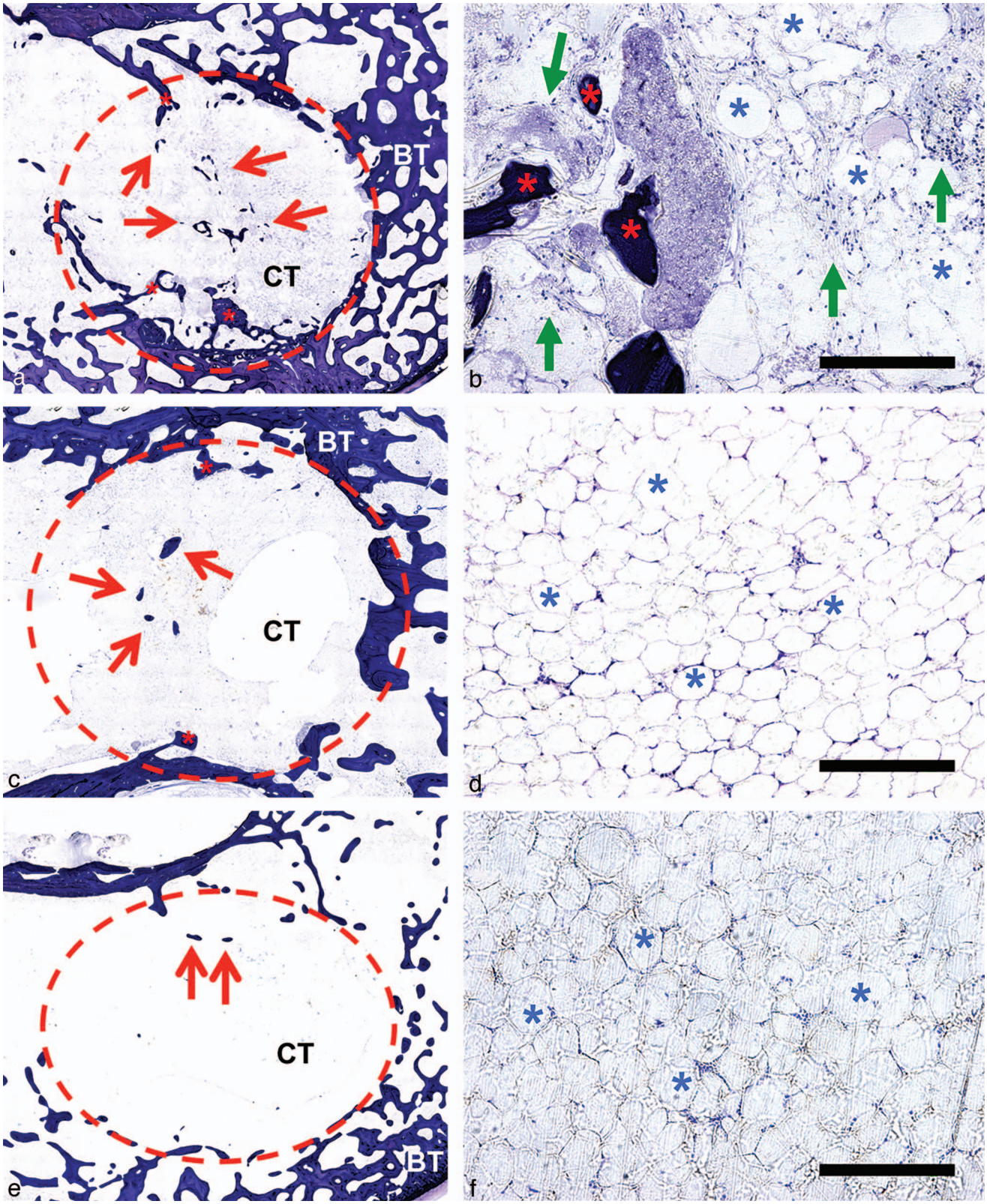

Figure 5. Postoperative course of the control defects in representative histological images. (a and b) The defect area (red dashed line in a) 1 month after the surgical treatment is shown. A low-grade growth of bone trabeculae (red asterisks) was visible starting from the bordering bone tissue (BT in a) of the defect areas, whereas only very few trabeculae (red arrows in a) were found within the defect center. In addition to the bone trabeculae (red asterisks), adipose cells/tissue (black arrows in b) and islands of connective tissue (green arrows in b) with mainly macrophages and granulocytes were detectable within the defect areas. (c and d) Histological images of the defect areas (red

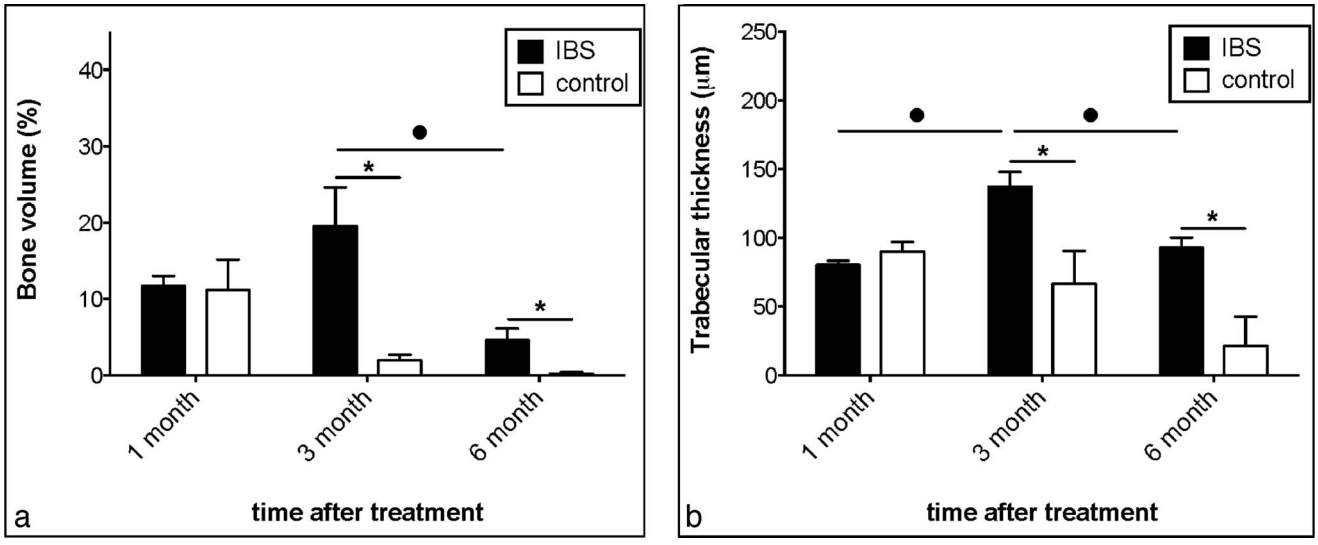

Figure 6. Results of the histomorphometrical measurements: (a) bone volume (in %) and (b) trabecular thickness (in μm) (*$P > .05$).

implantation without a premature ingrowth of connective tissue. Within this span, bone regeneration proceeded from the periphery of the bone defect and was accompanied by a degradation of the material, also towards the center of the implantation bed.

One month after application, histological analysis showed a peripheral osteoconductive growth of calcified bone tissue, while mostly uncalcified bone tissue was found in the central regions of the implantation bed. Interestingly, the bone growth process was found to be mediated by both components of the injected biomaterial, that is, the β-TCP granules and the hydrogel, and was especially prominent at this point. Thus, the regeneration process involved the β-TCP granules, which were integrated mainly within the calcified bone trabeculae in the peripheral regions of the implantation beds. By contrast, the guided growth of mainly uncalcified bone tissue in the central regions of the implantation bed was related mainly to the interspaces of the β-TCP granules that contained the hydrogel.

Three months after application, a substantial amount of newly formed bone was observable in the IBS group with a reduction in the biomaterial volume as an indication of its degradation. After 6 months, a nearly complete regeneration up to the state of restitutio ad integrum of the bone structure within the former defect areas was found, that is, a recovery of physiological trabecular structure and density. At this time point, no trace of the materials could be found radiographically in the IBS-treated group, while the histological analysis revealed the presence of very low amounts of the β-TCP granules, which were also shown to be involved in bone regeneration. Furthermore, histology revealed a vessel-rich granulation tissue composed mainly of monocytes, macrophages, and multinucleated giant cells within the implantation bed. This histological pattern indicates its cell-mediated degradation and has also been observed within the implantation bed of the same IBS within the subcutaneous tissue of the Wistar rat, as well as in the implantation beds of other synthetic biodegradable materials.[8,13–18,21] Interestingly, a peripheral trabecular bone structure was also found in the defect areas of the control groups 1 month after surgery, and this structure was comparable to the bone regeneration pattern observed in the group treated with the injectable bone substitute. However, only marginal bone growth was found after 3 and 6 months in the control group; thus, no adequate regeneration of the bone defects occurred.

These findings were also confirmed by histomorphometrical results, which revealed comparable amounts of bone volume and trabecular thickness in both study groups 1 month after surgery. Unfortunately, the observed uncalcified bone matrix in the central regions of the implantation beds of the IBS could not be included in the histomorphometrical analysis because the contrast of the toluidine blue staining was too low to separate this tissue component accurately from the surrounding connective tissue. Thus, it is presumed that the actual amount of newly built bone tissue in the IBS-treated group at this point was markedly higher compared with the bone growth in the control group. Interestingly, in the group treated with the IBS the peaks for bone volume and trabecular thickness were achieved 3 months after implantation, whereas after 6 months, a reduction in the bone volume was found,

←
dashed line in c) 3 months after surgery are shown. Only a few newly built bone trabeculae (red asterisks in c) were found at the borders of the defect area (red asterisks in c) growing out from the neighboring bone tissue (BT in c) and within the defect centers (red arrows in c) at this time point. The soft tissue within the defect areas was mainly composed of adipose cells (blue asterisks in d). (e and f) These images are representative of the tissue structure 6 months after surgical intervention. The overview of the defect area (red dashed line in e) showed only a very low presence of trabecular bone tissue (red arrows). The former defect area contained mainly adipose tissue (blue asterisks in f) (toluidine blue stainings; a, c, and e: excerpt of "total scans," magnification ×100; b, d, and f: magnification ×200, scale bars = 100 μm).

accompanied by complete regeneration of the bone defects. At these points, both histomorphometrical parameters showed significantly lower values for the control group, in which no defect regeneration was observed up to 6 months.

The presented results indicate that the IBS funtions as a placeholder within its implantation bed in the bone defects for up to 3 months after application. The ingrowth of calcified bone tissue was mainly related to the β-TCP granules, while the observed uncalcified and premature bone tissue was found within areas that included the hydrogel component hyaluronan. It is probable that the bone substitute material (especially the hydrogel component) allows the ingrowth of osteoblasts and the subsequent production of bone matrix. These results indicated that the material seems to function as a porous structure that supports the tissue-specific ingrowth of cells and matrix in addition to its physical feature as a filler that successfully prevents the premature ingrowth of connective tissue.

Furthermore, the histomorphometrical results obtained 1 month after treatment are interesting because the higher amounts of both calcified and uncalcified bone tissue in the group of the IBS are confirmed by the peak for bone tissue growth 3 months after surgery. These observations are related to a high activity of osteoblasts during this phase of bone regeneration, most probably induced by the hydrogel component and especially by hyaluronan, which has been shown to activate osteoblasts and inhibit osteoclasts.[22–25]

Furthermore, the decrease in bone growth that was found in the IBS group 6 months after treatment could be related to its nearly complete degradation. It was shown that only very low amounts of the small-sized β-TCP granules were histologically detectable after 6 months. Mechanistically, the attraction of osteoblasts could be reduced after 6 months on the basis of the fact that the IBS—particularly the polymer solution containing hyaluronan—appeared to be degraded faster than the β-TCP particles in vivo, as was also shown in previous studies.[8,20] Thus, the hydrogel content and especially hyaluronan as the inducer of the bone growth observed 1 and 3 months after material application seemed to be degraded, and the (bone) tissue distribution reverted to a "normal" physiological state.

To summarize, the presented results demonstrate the usefulness of the IBS based on β-TCP and a polymer solution composed of hyaluronan for the complete regeneration of bone defects within the time span of 6 months after its application. Therefore, the material was able to fulfill its roles as a placeholder and additionally as a scaffold-like structure in bone tissue repair. Moreover, the results of the present study help elucidate the regenerative mechanisms induced by the bone substitute material, which are the result of guided bone growth mediated by both the polymer component and the small-sized β-TCP particles. Thus, the materials function as a porous structure that supports the ingrowth of newly synthesized bone tissue. At the same time, the IBS undergoes degradation with time, beginning from the periphery of its implantation bed and progressing up to the central regions. Furthermore, no premature ingrowth of connective tissue was observed. Thus, the new IBS enables the induction of a guided integration and degradation behavior in accordance with the concept of GTR/GBR However, ongoing clinical studies in dental and orthopedic surgery will have to show to what extent the observed regenerative potential of the paste-like bone substitute material can be used for load-bearing and non-load-bearing bone defects.

Conclusions

The results of the present study show that the injectable bone substitute (IBS) based on beta-tricalcium phosphate (β-TCP), hyaluronan, and methylcellulose promotes the osteoconductive regeneration of critical-sized defects to a complete restitutio ad integrum of the femoral bone tissue after 6 months in accordance with the concept of GTR/GBR. In combination with directed material integration, a degradation process was found to take place from the periphery of the materials towards the center of the implantation bed over time, and a high implant bed vascularization was found. Therefore, the data presented here show that both the β-TCP component and the hydrogel component allow the combinational growth of bone tissue. Thus, this material combination appears to support a favorable matrix microenvironment for bone regeneration.

Abbreviations

β-TCP: beta-tricalcium phosphate
GTR/GBR: guided tissue regeneration/guided bone regeneration
IBS: injectable bone substitutes

References

1. Low KL, Tan SH, Zein SH, Roether JA, Mouriño V, Boccaccini AR. Calcium phosphate-based composites as injectable bone substitute materials. *J Biomed Mater Res B Appl Biomater*. 2010;94:273–286.

2. Lewis G. Injectable bone cements for use in vertebroplasty and kyphoplasty: state-of-the-art review. *J Biomed Mater Res B Appl Biomater*. 2006;76:456–468.

3. Larsson S, Hannink G. Injectable bone-graft substitutes: current products, their characteristics and indications, and new developments. *Injury*. 2011;42(Suppl 2):30–34.

4. Weiss P, Layrolle P, Clergeau LP, et al. The safety and efficacy of an injectable bone substitute in dental sockets demonstrated in a human clinical trial. *Biomaterials*. 2007;28:3295–3305.

5. Temenoff JS, Mikos AG. Injectable biodegradable materials for orthopedic tissue engineering. *Biomaterials*. 2000;21:2405–2412.

6. Sannino A, Demitri C, Madaghiele M. Biodegradable cellulose-based hydrogels: design and applications. *Materials*. 2009;2:353–373.

7. Gauthier O, Boix D, Grimandi G, et al. A new injectable calcium phosphate biomaterial for immediate bone filling of extraction sockets: a preliminary study in dogs. *J Periodontol*. 1999;70:375–383.

8. Ghanaati S, Barbeck M, Hilbig U, et al. An injectable bone substitute composed of beta-tricalcium phosphate granules, methylcellulose and hyaluronic acid inhibits connective tissue influx into its implantation bed in vivo. *Acta Biomater*. 2011;7:4018–4028.

9. Auger FA, Gibot L, Lacroix D. The pivotal role of vascularization in tissue engineering. *Annu Rev Biomed Eng*. 2013;15:177–200.

10. Kanczler JM, Oreffo RO. Osteogenesis and angiogenesis: the potential for engineering bone. *Eur Cell Mater*. 2008; 15:100–114.

11. Retzepi M, Donos N. Guided bone regeneration: biological principle and therapeutic applications. *Clin Oral Implants Res*. 2010;21:567–576.

12. Peters F, Reif D. Functional materials for bone regeneration from beta-tricalcium phosphate. *Materialwiss Werkst*. 2004;35:203–207.

13. Ghanaati S, Barbeck M, Orth C, et al. Influence of β-tricalcium

phosphate granule size and morphology on tissue reaction in vivo. *Acta Biomater*. 2010;6:4476–4487.

14. Ghanaati S, Barbeck M, Detsch R, et al. The chemical composition of synthetic bone substitutes influences tissue reactions in vivo: histological and histomorphometrical analysis of the cellular inflammatory response to hydroxyapatite, beta-tricalcium phosphate and biphasic calcium phosphate ceramics. *Biomed Mater*. 2012;7:015005.

15. Ghanaati S, Unger RE, Webber MJ, et al. Scaffold vascularization in vivo driven by primary human osteoblasts in concert with host inflammatory cells. *Biomaterials*. 2011;32:8150–8160.

16. Ghanaati S. Non-cross-linked porcine-based collagen I-III membranes do not require high vascularization rates for their integration within the implantation bed: a paradigm shift. *Acta Biomater*. 2012;8:3061–3172.

17. Barbeck M, Udeabor SE, Lorenz J, et al. Induction of multinucleated giant cells in response to small sized bovine bone substitute (Bio-Oss) results in an enhanced early implantation bed vascularization. *Ann Maxillofac Surg*. 2014;4:150–157.

18. Barbeck M, Udeabor S, Lorenz J, et al. High-temperature sintering of xenogeneic bone substitutes leads to increased multinucleated giant cell formation: in vivo and preliminary clinical results. *J Oral Implantol*. 2014;41: 212–222.

19. Ishikawa K. Calcium phosphate bone cement. In: Kokubo T, ed. *Bioceramics and Their Clinical Applications*. Philadelphia, Pa: Woodhead Publishing in Materials; 2008:438–463.

20. Krause M, Oheim R, Catala-Lehnen P, et al. Metaphyseal bone formation induced by a new injectable β-TCP-based bone substitute: a controlled study in rabbits. *J Biomater Appl*. 2014;28:859–868.

21. Anderson JM, Rodriguez A, Chang DT. Foreign body reaction to biomaterials. *Semin Immunol*. 2008;20:86–100.

22. Kawano M, Ariyoshi W, Iwanaga K, et al. Mechanism involved in enhancement of osteoblast differentiation by hyaluronic acid. *Biochem Biophys Res Commun*. 2011;405:575–580.

23. Pivetta E, Scapolan M, Wassermann B, Steffan A, Colombatti A, Spessotto P. Blood-derived human osteoclast resorption activity is impaired by Hyaluronan-CD44 engagement via a p38-dependent mechanism. *J Cell Physiol*. 2011;226:769–779.

24. Baud'huin M, Ruiz-Velasco C, Jego G, et al. Glycosaminoglycans inhibit the adherence and the spreading of osteoclasts and their precursors: role in osteoclastogenesis and bone resorption. *Eur J Cell Biol*. 2011;90:49–57.

25. Sasaki T, Watanabe C. Stimulation of osteoinduction in bone wound healing by high-molecular hyaluronic acid. *Bone*. 1995;16:9–15.